Jagannath University Journal of Science
Volume 07, Number I, December 2020, pp. 25-33
https://jnu.ac.bd/journal/portal/archives/science.jsp
ISSN 2224-1698

JnUJSci

# A Spectral Study on Transient Fluid Flow and Temperature Distribution through a Rotating Curved Rectangular Duct with Vortex Structure

**Research Article**

**Ratan Kumar Chanda, Bishnu Pada Ghosh, Sidhartha Bhowmick, Rabindra Nath Mondal***

*Department of Mathematics, Jagannath University, Dhaka, Bangladesh*

**Received: 01 October 2020**
**Accepted: 02 December 2020**

**Abstract:** Fluid flow through a curved rectangular duct (CRD) in a rotating system is investigated numerically. The lower edge of the working system is considered to be heated while the top edges in cold; the remaining walls are well insulated. The controlling parameters of the fluid are the rotating parameter *Tr*, the Grashof number *Gr*, the Prandtl number *Pr*, and the pressure gradient parameter *Dn*. The existing system is rotated about the center of curvature both clockwise and anti-clockwise direction over a wide range *Tr* for $-2000 \le Tr \le 2000$. Newton-Raphson iteration method as well as path continuation technique is used to compute steady solutions (SS). The computational effort demonstrates that four branches of axisymmetric steady solutions with 2-to 10-vortex are obtained. For an increasing *Tr* in the co-rotating direction, the transient flow develops in the consequence "*chaotic* → *multi-periodic* → *steady-state*"; for counter rotating case, the chaotic flow turns into steady-state via multi-periodic oscillation. Secondary flow patterns and temperature profiles have also been investigated where there exist two- to multi-vortex solutions. We investigated the dependence of heat transfer (HT) on the Taylors number and thermal bounding condition and the present study shows that the secondary flow provided a promotion of convective heat transfer (CHT);and the chaotic flow that arises relatively at small *Tr*, impacts on HT stronger and more effectively than other physically realizable solutions.

**Keywords:** *Curved duct ● Steady solution ● Secondary flow ●Time progression ● Phase space ● Heat transfer*

## 1. Introduction

The development of fluid flows and enhancement in HT through CRDs or channels in a rotating system has been drawn great attention in research and practice by many researchers for a vast range of engineering application for example flow separation, heating and cooling system, solar energy, electric generators, rocket engine and many more. The existence of such problem was first analyzed in detail in 1927, called the pioneer, when Dean (1927) described what he gave attention as a flow condition curiosity. Ever since, several researchers have done many significant studies. The researchers are mentioned to Ligrani and Niver (1988) and Berger *et al*. (1983) for a number of exceptional reviews on curved duct flows.

It has been established that in a rotating curved system, two forces, namely, Coriolis and Centrifugal act on the fluid. The resulting two forces impact the fluid flow and create the swirling and axial flow accordingly. A detailed pore-scale study on such systems under spectral based method for counter and co-rotating of the curved square duct (CSD) system is available in literature (Mondal *et al*. 2014) and studied solution structure, stability and transitions of the flow. The close bonding to the transient behavior and the bifurcation structure among steady

* Corresponding author: Rabindra Nath Mondal
*Email address:* rnmondal71@yahoo.com

branches is also shown in the study of Mondal *et al.* (2007). The review article by Selmi *et al.* (1994) has described the resulting effects on the bifurcation structure of 2-D flows in a rotating curved duct (CD). Adopting spectral method in a rotating CSD, Yamamoto *et al.* (1999) investigated the flow formation and found a 6-cell phenomenon of the swirling flow.

The understanding of the unsteady flow behaviors is of fundamental importance. Wang and Yang (2005) studied numerically and empirically the periodic fluctuations for an incompressible fluid in a CSD and the comparison shows an excellent agreement between the both results. Chandratilleke and Nursubyak (2003) performed numerical approach to elucidate the flow properties through the variable geometries of different aspect ratios where heated the outer edge. Mondal *et al.* (2013) conducted numerical manner to analyze the flow transition in CD. They investigated the impacts of *Dn* and *Gr* number on the secondary flow pattern. Islam *et al.* (2017) deliberated the influence of Dean numbers over a wide range of *Tr* on transition in a rotating CRD flows. However, most of the relevant studies only focused on the weak rotational speed, while the transient solution with coupled impacts on buoyancy-influenced centrifugal-Coriolis instabilities through a rotating CRD for highly gyratory speed are not considered though it has numerous engineering applications. Hence, motivated from these unresolved issues, the present study deals with the effects of high gyration and curvature on unsteady fluid flow in a CRD.

To progress the conception of thermo-fluid behavior and CHT in a CD, Chandratilleke and Nursubyakto (2003) disclosed that the CHT at the outer wall of the CD is more capable than that in a SD and the contribution of Dean vortices is to promote HT in CD. Yanase *et al.* (2002) and Mondal *et al.* (2014) performed numerical simulation to study the fluctuation behavior of the flow through a CRD/SD and recognized that SFs boost HT in the flow. Recently, Hasan *et al.* (2019a, 2019b) conducted numerical approach of fluid flow and HT through a rotating CSD for various curving. They performed positive rotating case and investigated combined impacts of the centrifugal, Coriolis and buoyancy forces. They showed time-progression flow experiences via different flow unsteadiness. Very recently, Roy *et al.* (2020) applied spectral method to predict hydrodynamic instability and CHT through a rotating CRD of moderate curvature. They obtained three branches of steady solutions and showed the various flow state for increasing positive *Tr*. The key intention of the current study is to examine the perplexing flow behavior and energy distribution in a tightly coiled rectangular duct with stream-wise curvature while identifying the influence from various flow and geometrical parameters. In the present study, flow structure as well as transient flow characteristics with CHT through a rotating CRD with strong rotational speed is investigated.

## 2. Physical Problem and Governing Equations

Consideration is given for fully developed 2D flow which passes through a CRD. Figure 1 illustrates the cross-sectional view and the coordinate system of the computational domain with necessary notations. The system rotates with the angular velocity $\Omega_T$ around the $y'$ axis. The bottom edge of the working system is considered to be heated while the upper edges in normal room warmth; the remaining walls are well insulated to prevent any heat loss. The fluid passes through uniformly in the stream-wise direction as exhibited in Figure 1.

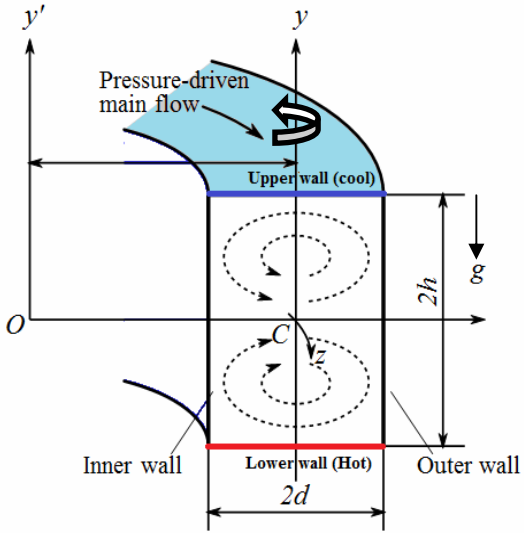


**Figure 1:** Geometry of the problem

The dimensional variables are non-dimensionalized by using the representative length and the representative velocity, which are not shown here for brevity. The stream functions for cross-sectional velocities have the following form

$$u = \frac{1}{1+\delta x}\frac{\partial \psi}{\partial y} \quad \text{and} \quad v = -\frac{1}{1+\delta x}\frac{\partial \psi}{\partial x} \tag{1}$$

Then, basic equations for the axial velocity ($w$), stream function ($\psi$), and temperature ($T$) are derived from the Navier–Stokes equations and energy equation as follows

$$(1+\delta x)\frac{\partial w}{\partial t} = Dn + (1+\delta x)\Delta_2 w - \frac{1}{2}\frac{\partial(w,\psi)}{\partial(x,y)} - \frac{\delta^2 w}{1+\delta x} - \frac{\delta}{2(1+\delta x)}\frac{\partial \psi}{\partial y}w + \delta\frac{\partial w}{\partial x} - \delta Tr\frac{\partial \psi}{\partial y} \tag{2}$$

$$\left(\Delta_2-\frac{\delta}{1+\delta x}\frac{\partial}{\partial x}\right)\frac{\partial\psi}{\partial t}=-\frac{1}{2(1+\delta x)}\frac{\partial(\Delta_2\psi,\psi)}{\partial(x,y)}$$
$$+\frac{\delta}{2(1+\delta x)^2}\left[\frac{\partial\psi}{\partial y}\left(2\Delta_2\psi\right)-\frac{3\delta}{1+\delta x}\frac{\partial\psi}{\partial x}+\frac{\partial^2\psi}{\partial x^2}\frac{\partial\psi}{\partial x}\frac{\partial^2\psi}{\partial x\partial y}\right]$$
$$+\frac{\delta}{(1+\delta x)^2}\times\left[3\delta\frac{\partial^2\psi}{\partial x^2}-\frac{3\delta^2}{1+\delta x}\frac{\partial\psi}{\partial x}\right]-\frac{2\delta}{1+\delta x}\frac{\partial}{\partial x}\Delta_2\psi$$
$$+w\frac{1}{2}\frac{\partial w}{\partial y}+\Delta_2{}^2\psi+\frac{1}{2}Tr\frac{\partial w}{\partial y} \quad (3)$$

$$\frac{\partial T}{\partial t}=\frac{1}{\mathrm{Pr}}\left(\Delta_2 T+\frac{\delta}{1+\delta x}\frac{\partial T}{\partial x}\right)-\frac{1}{2(1+\delta x)}\frac{\partial(T,\psi)}{\partial(x,y)} \quad (4)$$

The system is therefore governed by four non-dimensional parameters, the Dean number *Dn*, the Taylor number *Tr*, the Grashof number *Gr* and the Prandtl number Pr, which are included in equations (2) - (4) defined as

$$\left.\begin{aligned} Dn&=\frac{Gd^3}{\mu\upsilon}\sqrt{\frac{2d}{L}},\ Gr=\frac{\beta g\Delta T d^3}{\upsilon^2}\\ Tr&=\frac{2\sqrt{2\delta}\Omega_T d^3}{\upsilon\delta},\ \mathrm{Pr}=\frac{\upsilon}{\kappa}\end{aligned}\right\} \quad (5)$$

The applied boundary conditions for $w$ and stream function:

$$\left.\begin{aligned} w(\pm1,y)=w(x,\pm1)=\psi(\pm1,y)=\psi(x,\pm1)=0\\ \frac{\partial\psi}{\partial x}(\pm1,y)=\frac{\partial\psi}{\partial y}(x,\pm1)=0\end{aligned}\right\} \quad (6)$$

Boundary condition for temperature *T:*

$$T(x,1)=1,T(x,-1)=-1,T(\pm1,y)=-y \quad (7)$$

## 3. Numerical Procedure

### 3.1 Method of numerical procedure

For finding the numerical result from the equations (2) to (4), spectral method (Gottlieb and Orazag, 1977) is applied at the obtained dimensionless momentum and energy equations. According to the principle of this scheme, the variables are expanded in a series functions consisting of the Chebyshev polynomials. That is, the functions expansion of $\varphi_n(x)$ and $\psi_n(x)$ are articulated as

$$\left.\begin{aligned} \varphi_n(x)&=(1-x^2)C_n(x),\\ \psi_n(x)&=(1-x^2)^2C_n(x)\end{aligned}\right\} \quad (8)$$

where, $C_n(x)=\cos\left(n\cos^{-1}(x)\right)$ is the $n^{\text{th}}$ order Chebyshev polynomial. $w(x,y,t)$, $\psi(x,y,t)$ and $T(x,y,t)$ are expanded in terms of $\varphi_n(x)$ and $\psi_n(x)$ as

$$\left.\begin{aligned} w(x,y,t)&=\sum_{m=0}^{M}\sum_{n=0}^{N}w_{mn}(t)\varphi_m(x)\varphi_n(y)\\ \psi(x,y,t)&=\sum_{m=0}^{M}\sum_{n=0}^{N}\psi_{mn}(t)\psi_m(x)\psi_n(y).\\ T(x,y,t)&=\sum_{m=0}^{M}\sum_{n=0}^{N}T_{mn}(t)\varphi_m(x)\varphi_n(y)-y\end{aligned}\right\} \quad (9)$$

where *M* and *N* represent the truncation numbers in the *x*- and *y*-directions respectively, and $w_{mn}$, $\psi_{mn}$ and $T_{mn}$ are the coefficients of expansion. The collocation points $\left(x_i,y_j\right)$ are taken to be

$$x_i=\cos\left[\pi\left(1-\frac{i}{M+2}\right)\right],\ y_j=\cos\left[\pi\left(1-\frac{j}{N+2}\right)\right] \quad (10)$$

where $i=1,\ldots,M+1$ and $j=1,\ldots,N+1$. To attain time dependent evolution of $\overline{w}(x,y)$, $\overline{\psi}(x,y)$ and $\overline{T}(x,y)$ the necessary series expansion (9) is then substituted into the basic equations (2) - (4) abide by applying the collocation method. Finally, in order to calculate the unsteady solutions, the Crank-Nicolson and Adams-Bashforth methods together with the function expansion (9) and the collocation methods are applied to Eqs. (2) to (4).

### 3.2 Resistance coefficient

The resistant coefficient $\lambda$, called the *hydraulic resistance coefficient*, representing the dimension of the flow state, clarified as

$$\frac{p_1^*-p_2^*}{\Delta_{z^*}}=\frac{\lambda}{d_h^*}\frac{1}{2}\rho\left\langle\omega^*\right\rangle^2 \quad (11)$$

where $\langle\ \rangle$ positions for the mean over the cross-section of the duct and $d_h^*$; hydraulic diameter, $\rho$; density, $P_1^*$; upstream pressure and $P_2^*$; downstream pressure and $\left\langle\omega^*\right\rangle$; stream-wise main velocity deliberated by

$$\langle\omega^*\rangle=\frac{v}{4\sqrt{2\delta d}}\int_{-1}^{1}dx\int_{-1}^{1}\omega(x,y,t)\,dy \quad (12)$$

$\lambda$ is linked to the mean dimensionless axial velocity as

$$\lambda = \frac{16\sqrt{2\delta}Dn}{3\langle w\rangle^2}. \quad (13)$$

where $\langle w\rangle = \sqrt{2\delta}d\langle w^*\rangle/\upsilon$.

## 4. Results and Discussion

### 4.1 Steady solutions

A detailed investigation of the combined flow structure in the steady solution (SS) branch is carried out and discuss the flow configurations on various steady branches. The simulations are performed in the following range of governing parameters as shown in Table 1. With the ongoing numerical approach, four branches of asymmetric SS are obtained for the positive rotation. A branching pattern of SS is revealed in Fig. 2. As seen in Fig. 2, the four branches are differentiated by different colors and line of patterns. The four SS branches are named the 1st, 2nd, 3rdand 4th steady branch respectively. It is seen that there is no bifurcating connectivity among the branches of steady solutions.

**Table 1:** Range of governing parameters considered in the simulations.

| | |
|---|---|
| Grashof number ($Gr$) | 100 |
| Dean number ($Dn$) | 1000 |
| Curvature ($\delta$) | 0.1 |
| Tylor number ($Tr$) | $-2000 \le Tr \le 2000$ |
| Prandtl number (Pr) | 7.0 |

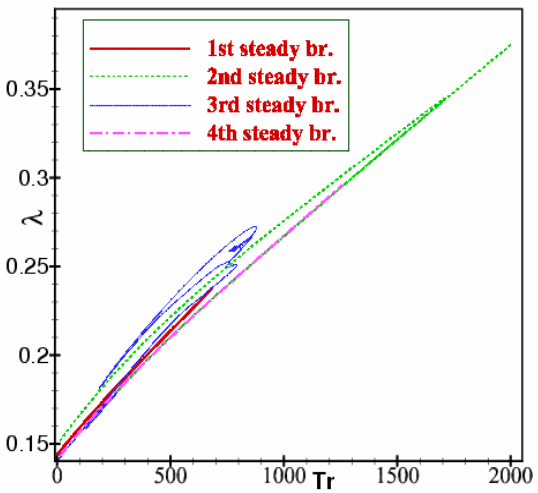


**Figure 2:** Branching structure of steady solutions for positive rotation

Figure 3 shows pattern of SFs, temperature profile and axial flow distributionfor the respective four branches. It is clearly observed from Fig. 3 that the SF is an symmetric and axisymmetric 2- and 4-vortex on the first and second branches; 2- to10-vortex on the third branch while only 2-vortex on the fourth SS branch.

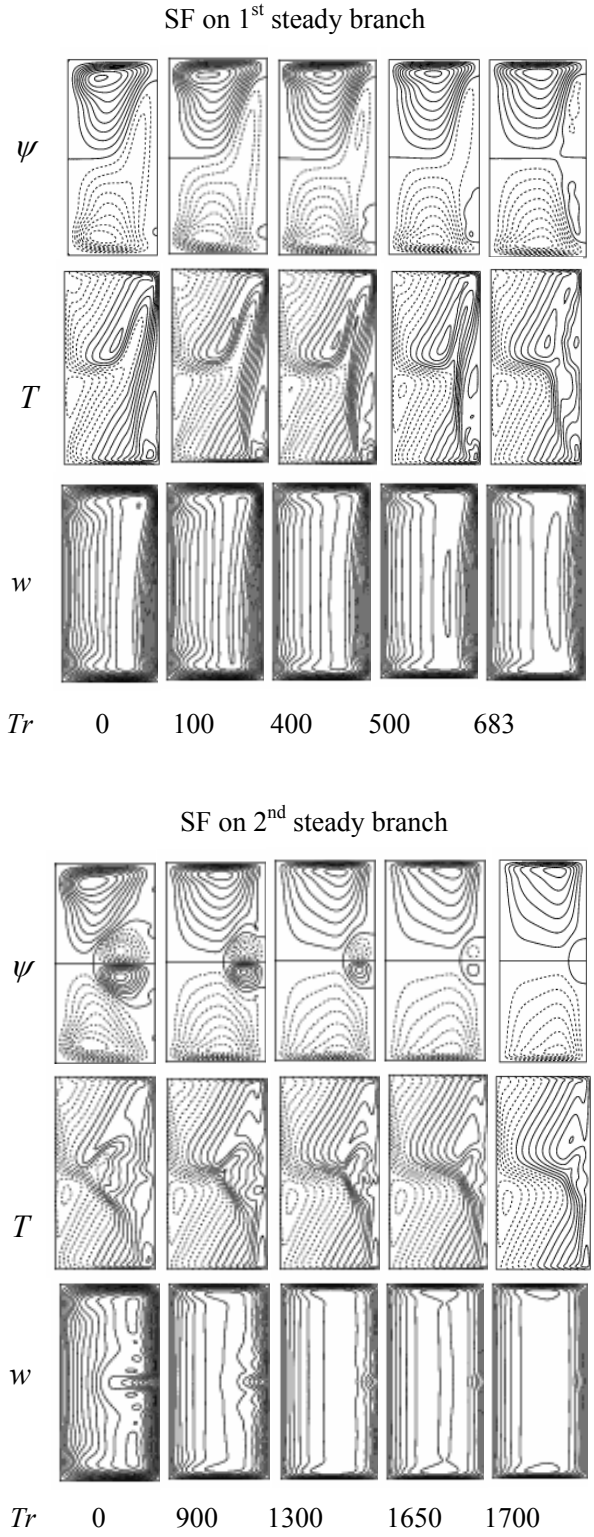

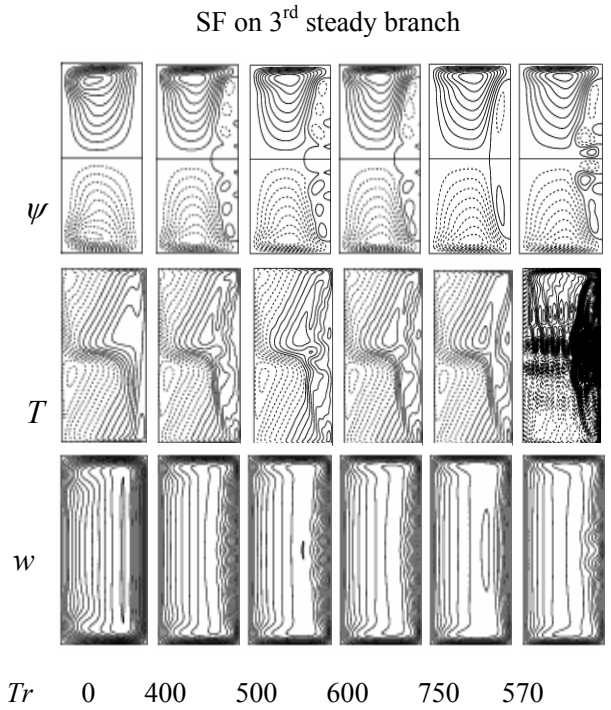


**Figure 3:** Velocity contours (top & bottom) of the secondary flow (SF) and axial flow and isotherm (middile) for various values of *Tr* on various branches of steady solutions.

### 4.2 Oscillating behavior and power spectrum

#### 4.2.1 Case I: Positive rotation ( $0 \le Tr \le 2000$ )

In this subsection, a detailed discussion of the results of oscillating behavior for various regimes of *Tr* ranging from 0 to 2000 keeping at $\delta = 0.1$ , *Gr* = 100 and *Dn* = 1000 and the flow state is justified by the power spectrum (PS) density and analysis of the frequency signal. We calculate the oscillating behavior for *Tr* = 0 as depicted Fig. 4 (a). It is seen that the unsteady flow (UF) fluctuates haphazardly i.e. the flow is chaotic for *Tr* = 0. To be confirm whether the flow is chaotic or not by sketching the PS as presented in Fig. 4(b). Figure 4(c) represents the vortex-structure and isotherm where we see that the chaotic flow oscillates sporadically in the axisymmetric 4- to 6-vortex solution for *Tr* = 0. When the value of *Tr* is gradually increased, at *Tr* = 1498.5, a multi-periodic oscillation takes place at *Tr* = 1498.5 with asymmetric 3- to 5-vortex solution (refer to Figs. 5(a) and 5(c)). PS diagrams to clearly showcase the multi-periodicity feature at *Tr* = 1498.5 is presented in Fig. 5 (b). With further increase of *Tr*, another flow transformation occurs at *Tr* = 2000 where the multi-periodic state transformed into a steady-state with axisymmetric 2-vortex solution (refer Figs. 6(a) and 6(b)).

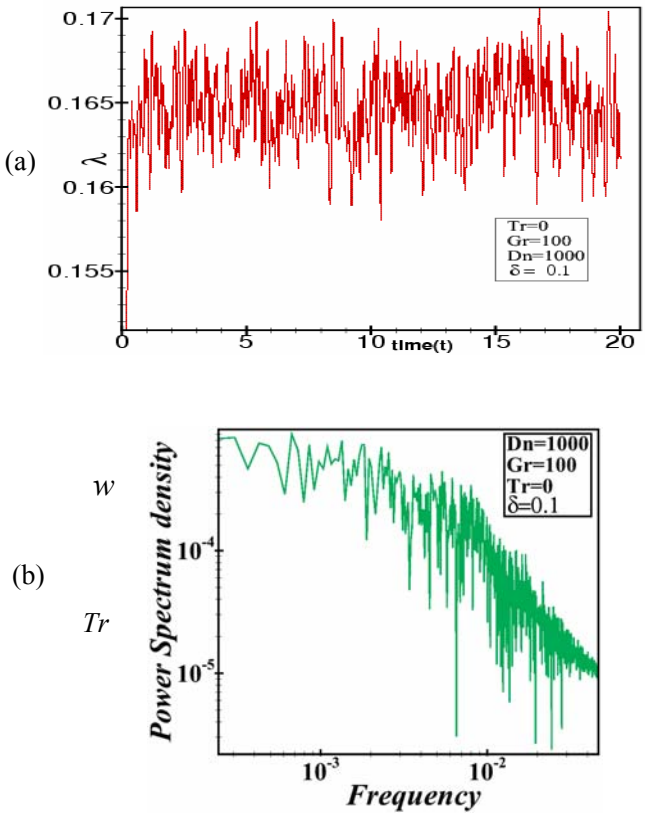

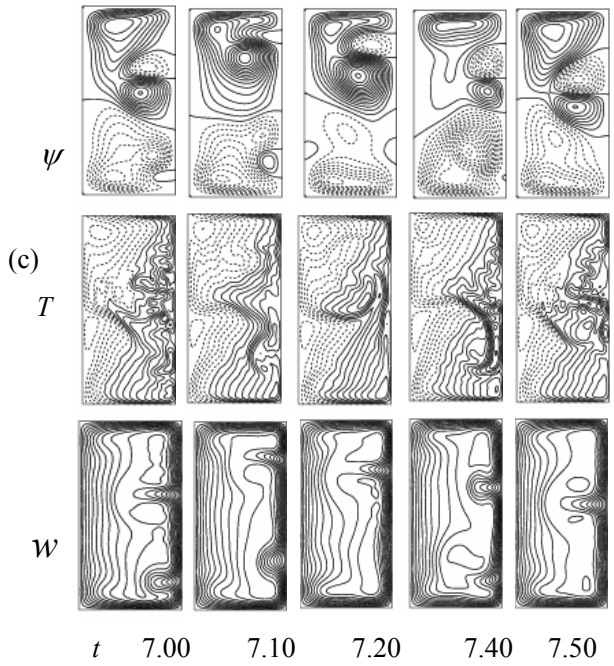


**Figure 4:** Transient solution for $Tr = 0$. (a) $\lambda$ as a function of time, (b) Power-spectrum (c) Velocity contour (top & bottom) and isotherm (middle) for $7.00 \le t \le 7.50$.

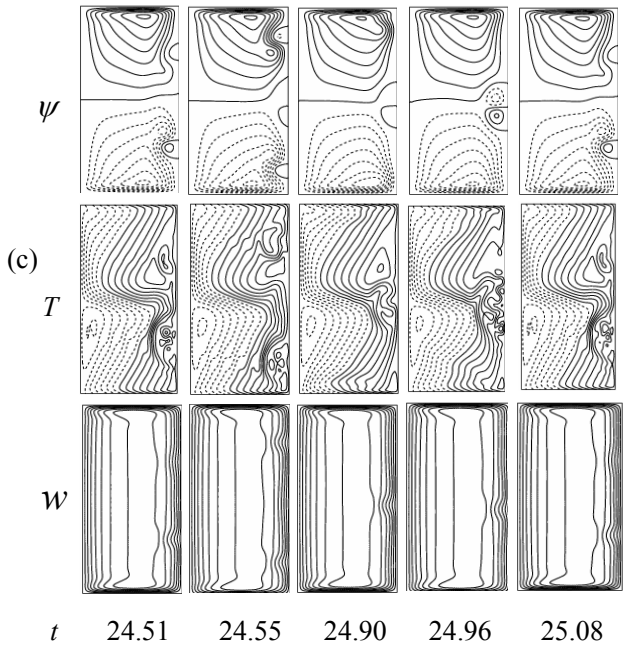


**Figure 5:** Transient solution for $Tr = 1498.5$. (a) $\lambda$ as a function of time, (b) Power-spectrum (c) Velocity contour (top & bottom) and isotherm (middle) for $24.51 \le t \le 25.08$.

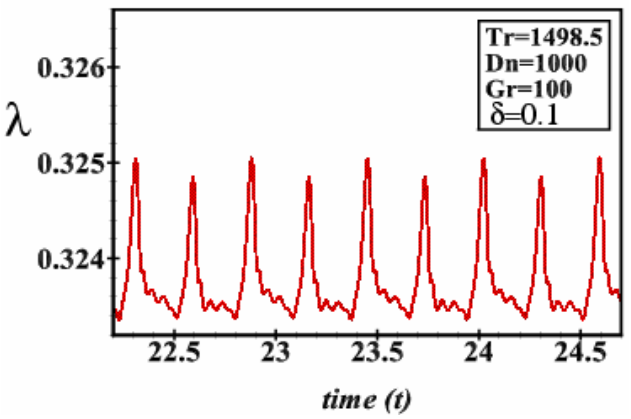


(a)

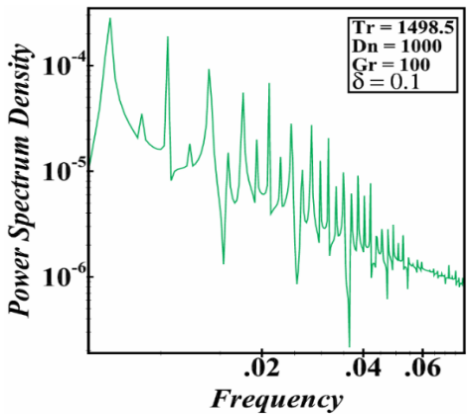


(b)

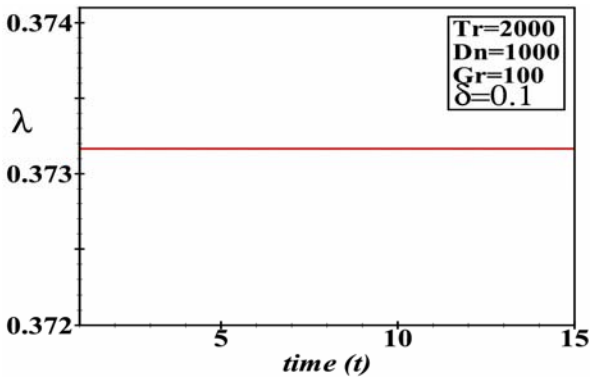


(a)

$t = 11.00$

(b)

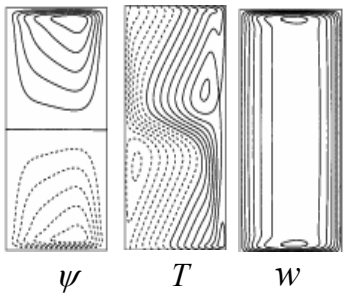


**Figure 6:** Transient solution for $Tr = 2000$. (a) $\lambda$ as a function of time, (b) Velocity contour (left & right) and isotherm (middle) for $t = 11.00$.

**4.2.2** Case **II: Negative rotation (** $-2000 \le Tr \le 0$ **)**

Here, we investigated oscillating behavior for negative rotation at $-2000 \le Tr \le 0$ and $\delta = 0.1$. Dimensionless parameters representing the Grashof number; *Gr*, the Dean number; *Dn* and curvature are set as 100, 1000 and 0.1 respectfully. The flow oscillates irregularly for *Tr* = -10 i.e. the flow is chaotic with 3 to 4-vortex solution as evidenced by Figs. 7(a) and 7(c). We plot PS to pronounce more clearly as shown in Fig. 7(b). On further increasing the value of *Tr* in the negative direction, multi-periodic flow pattern with axisymmetric 6-vortex is observed which is well justified by PS diagram at *Tr* = -1250 as presented in Fig. 8(b). It is clearly observed from Figs. 9(a) and 9(b) that the flow structure is steady-state with axisymmetric 2-vortex solution at *Tr* = -2000. When the Dean vortices that get generated adjacent to the concave wall of the duct and if the SF becomes stronger, then heat transfer occurs at a great deal than usual. In this study, temperature distributions show that the streamlines of the heat flow is uniformly distributed to all parts of the contour transferring heat from bottom wall to the fluid, and the contribution of the rotation and pressure on secondary flows significantly change and increase the number of secondary vortices.

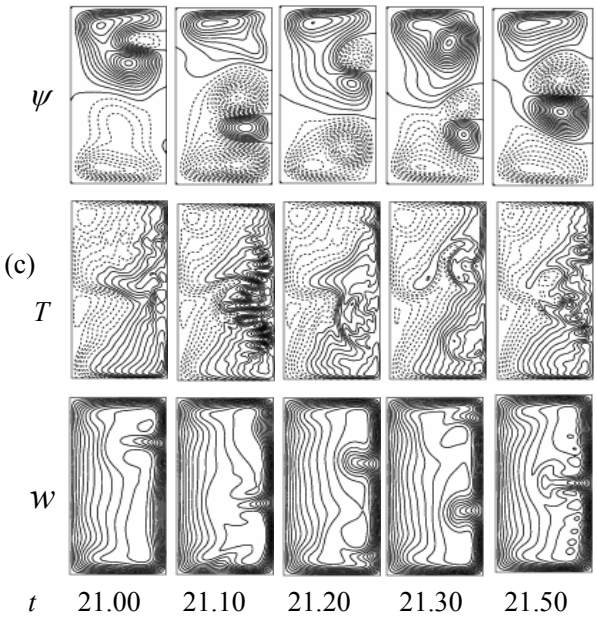


**Figure 7:** Transient solution for *Tr* = -10. (a) $\lambda$ as a function of time, (b) Power-spectrum (c) Velocity contour (top & bottom) and isotherm (middile) for $21.00 \le t \le 21.50$

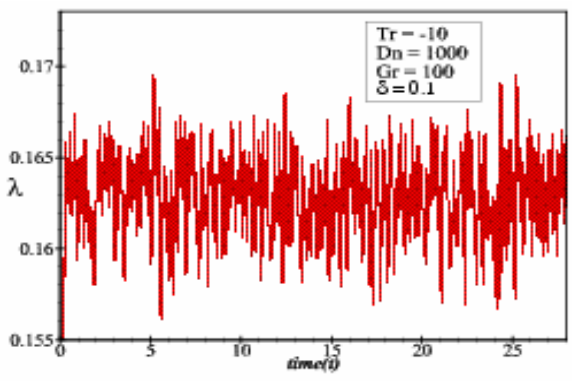


(a)

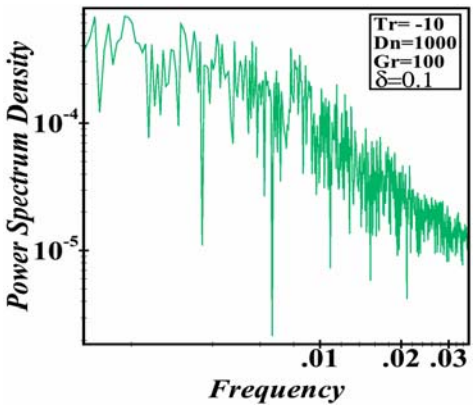


(b)

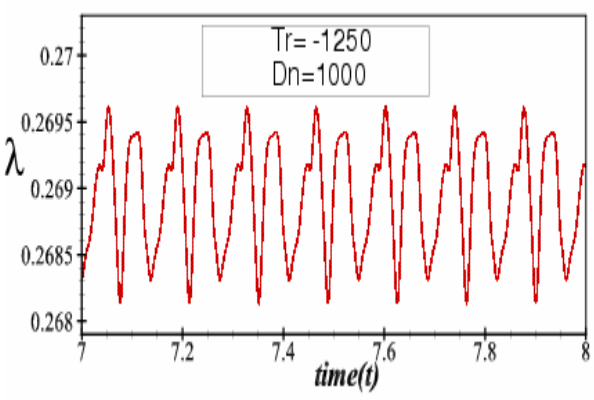


(a)

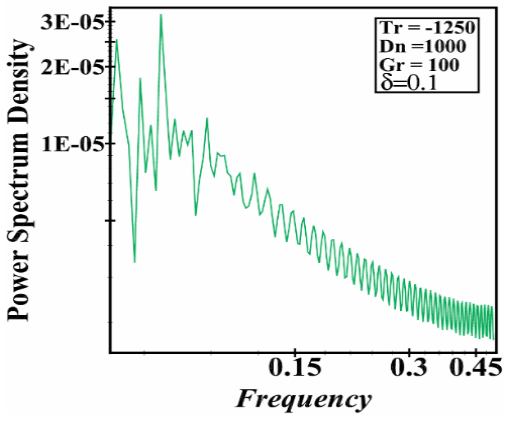


(b)

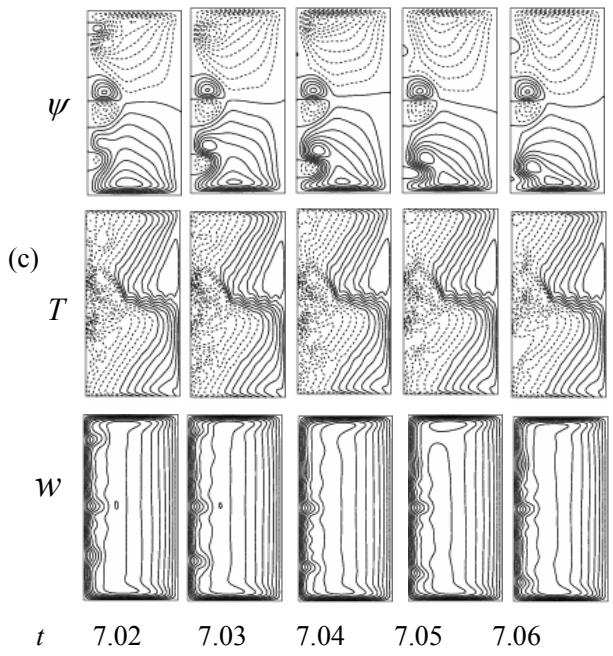


**Figure 8:** Transient solution for $Tr$ = -10. (a) $\lambda$ as a function of time, (b) Power-spectrum (c) Velocity contour (top & bottom) and isotherm (middile) for $7.02 \le t \le 7.06$.

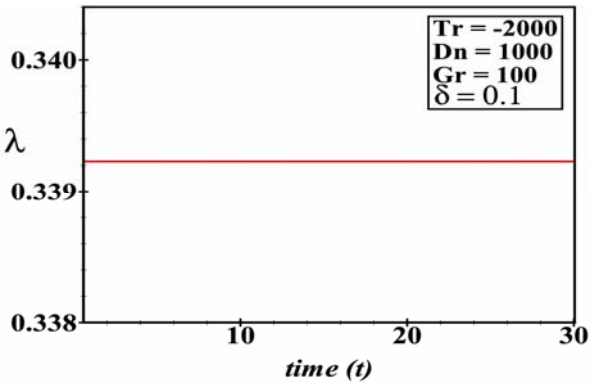


(a)

$t$ =20.00

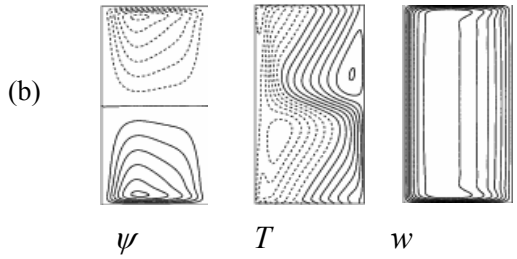


**Figure 9:** Transient solution for $Tr$ = 2000. (a) $\lambda$ as a function of time, (b) Velocity contour (left & right) and isotherm (middile) for $t$ = 20.00.

### 4.3 Vortex-structure for transient solutions

To observe vortices of SF, here we show vortex diagram of SF as a function of $Tr$ with the curvature is shown in Fig. 10 for $0 \le Tr \le 2000$ and $0.001 \le \delta \le 0.5$ .The structural response of the vortex can be observed:

(i) SF is a 2- to 12-vortex mode; (ii) the highest number12- and 8-vortex mode are displayed at $\delta = 0.001$ for $Tr = 100$ and $Tr = 1250$ respectively, while 4- and 2-vortex at $\delta = 0.1$ and $\delta = 0.5$ respectively. Therefore, it may be suggested that, the enhancement of heat transfer for chaotic flow is more effective than other flow state as a result the number of Dean vortices generated near outer edge for this flow, which match well with the literature in numerical result (Razavi *et al.* 2015) in a rotating curved duct.

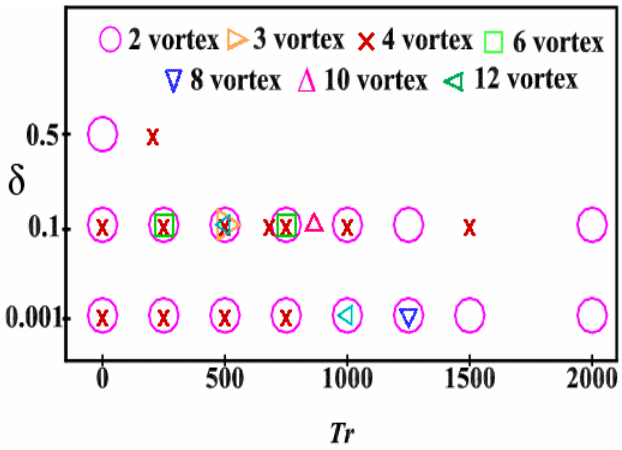


**Figure 10:** Schematic diagram of the observed SFs for $0.001 \le \delta \le 0.5$ and $0 \le Tr \le 2000$.

## 5. Conclusion

The ongoing study determines a spectral-based numerical analysis of flow characteristics and heat transfer performance in a curved rectangular geometry of aspect ratio 2 and curvature ratio ranging from 0.001 to 0.5 at rotating conditions which was investigated numerically over a wide range of rotating speed varying from -2000 to 2000.The temperature difference was created between lower and upper edges of the duct. The followings are the major findings as found in the present study:

- An asymmetric four branches of SS are found with 2- to 10-vortex on various branches.
- Time-progression as well as PS analysis demonstrates that transient flow develops in the consequence "*chaotic → multi-periodic → steady-state*", for counter rotating case; for co-rotating case, however, the flow experiences "*chaotic → multi-periodic → steady-state*".

- Velocity contours show that there exists axisymmetric 2-vortex solution for the steady-state, 3- to 6-vortex and 4- to 6-vortex solutions for the multi-periodic and chaotic oscillation respectively.

- Convective heat transfer is increased with the increase of rotation. The highly complex secondary flow filed is developed with higher *Tr* and HT is boosted substantially by the chaotic solutions than the other flow state.

**References**

Berger SA, Talbot L and Yao LS. 1983. Flow in Curved Pipes, *Annual. Rev. Fluid. Mech*. 5: 461-512.

Chandratilleke TT and Nursubyakto K. 2003. Numerical Prediction of Secondary Flow and Convective Heat Transfer in Externally Heated Curved Rectangular Ducts. *Int. J. Thermal Sciences* 42: 187-198.

Dean WR. 1927. Note on the Motion of Fluid in a Curved Pipe. *Philos Mag*. 4: 208-223.

Gottlieb D and Orazag SA. 1977. Numerical Analysis of Spectral Methods. *Society for Industrial and Applied Mathematics*, Philadelphia, USA.

Hasan MS, Mondal RN and Lorenzini G. 2019a. Numerical Prediction of Non-isothermal Flow with Convective Heat Transfer through a Rotating Curved Square Channel with Bottom Wall Heating and Cooling from the Ceiling. *Int. J. Heat and Technology* 37(3): 710-720.

Hasan MS, Mondal RN and Lorenzini G. 2019b. Centrifugal Instability with Convective Heat Transfer through a Tightly Coiled Square Duct. *Mathematical Modelling of Engineering Problems* 6(3): 397-408.

Islam MZ, Mondal RN and Rashidi MM. 2017. Dean-Taylor Flow with Convective Heat Transfer through a Coiled Duct. *Computers and Fluids* 149: 41-55.

Ligrani PM and Niver RD. 1988. Flow Visualization of Dean Vortices in a Curved Channel with 40 to 1 Aspect Ratio. *Physics of Fluids* 31(12): 3605.

Mondal RN, Ray SC and Islam S. 2014. Solution Structure, Stability and Pattern Variation of Secondary Flows through a Rotating Curved Duct with Rectangular Cross-section. *International Journal of Energy & Technology* 6(5): 1-12.

Mondal RN, Kaga Y, Hyakutake T and Yanase S. 2007. Bifurcation Diagram for Two-dimensional Steady Flow and Unsteady Solutions in a Curved Square Duct. *Fluid Dynamics Research* 39: 413-446.

Mondal RN, Islam MS, Uddin K and Hossain MA. 2013. Effects of Aspect Ratio on Unsteady Solutions through Curved Duct Flow. *Applied Mathematics and Mechanics* 34(9): 1107–1122.

Mondal RN, Ray SC and Yanase S. 2014. Combined Effects of Centrifugal and Coriolis Instability of the Flow through a Rotating Curved Duct with Rectangular Cross Section. *Open Journal of Fluid Dynamics* 4: 1-14.

Razavi SE, Soltanipour H and Choupani P. 2015. Second Law Analysis of Laminar Forced Convection in a Rotating Curved Duct. *Thermal Sciences* 19(1): 95-107.

Roy SC, Hasan MS and Mondal RN. 2020. On the Onset of Hydrodynamic Instability with Convective Heat Transfer through a Rotating Curved Rectangular Duct. *Mathematical Modelling of Engineering Problems* 7(1): 31-44.

Selmi M, Nandakumar K and Finlay WH.1994. A Bifurcation Study of Viscous Flow through a Rotating Curved Duct. *J. Fluid Mechanics* 262: 353-375.

Wang L and Yang T. 2005. Periodic Oscillation in Curved Duct Flows. *Physica D* 200: 296-302.

Yamamoto K, Yanase S and Alam MM. 1999. Flow through a Rotating Curved Duct with Square Cross-section. *J. Phys. Soc. Japan* 68: 1173-1184.

Yanase S, Kaga Y and Daikai R. 2002. Laminar Flow through a Curved Rectangular Duct over a Wide Range of the Aspect Ratio. *Fluid Dynamics Research* 31: 151-183.